

First-principles investigation of lattice thermal conductivity and structural stability of $\text{CH}_3\text{NH}_3\text{PbI}_3$

Ibrahim Omer Abdallah^{1,2}, Daniel P Joubert¹, and Mohammed S H Suleiman^{1,3}

¹ The National Institute for Theoretical Physics, School of Physics and Mandelstam Institute for Theoretical Physics, University of the Witwatersrand, Johannesburg, Wits 2050, South Africa.

² Department of Scientific Laboratories, Sudan University of Science and Technology, Khartoum, Sudan.

³ Department of Basic Sciences, Imam Abdulrahman Bin Faisal University, P. O. Box 1982, Dammam, KSA.

E-mail: ibrphysics@gmail.com

Abstract. Hybrid halide perovskites have recently emerged as new materials for solar cell applications leading to a new class of hybrid semiconductor photovoltaic cells, with very recent results demonstrating a 20.1% efficiency. Here, we investigate the structural stability, elastic constants, vibrational properties and lattice thermal conductivity of the orthorhombic $\text{CH}_3\text{NH}_3\text{PbI}_3$ using first-principles density functional theory calculations. The relaxed system is dynamically stable, while the equilibrium elastic constants satisfy all the mechanical stability criteria for orthorhombic crystals, showing stability against the influence of external forces. The non-isotropic lattice thermal conductivity of $\text{CH}_3\text{NH}_3\text{PbI}_3$ was calculated with the single-mode relaxation-time approximation and a full solution of the linearized phonon Boltzmann equation from first-principles anharmonic lattice dynamics calculations. Our results show that lattice thermal conductivity is anisotropic, and the calculated lattice thermal conductivity at 150 K was found to be 0.189, 0.138, and 0.530 $\text{Wm}^{-1}\text{K}^{-1}$ in the directions x , y and z , respectively

1. Introduction

Hybrid organic-inorganic perovskites have recently attracted strong interest as photo absorbers in solar cells, due to their high absorption coefficient, high carrier mobility, long diffusion lengths and ease of fabrication [1, 2]. Methyl ammonium lead iodide $\text{CH}_3\text{NH}_3\text{PbI}_3$ is one of the most relevant for photovoltaic applications in the perovskite family. Depending on temperature and on atomic sizes of the chemical constituents, perovskites can possess cubic, tetragonal or orthorhombic structural phases. For temperatures below 160 K, the $\text{CH}_3\text{NH}_3\text{PbI}_3$ perovskite structure presents an orthorhombic crystal symmetry with space group Pnma (62) [3]. Brevio F. et al., [4] and Feng [5] have identified the lattice dynamics, vibrational spectra and the mechanical properties of the cubic, tetragonal and orthorhombic phases. However, to the best of our knowledge, the vibrational and elastic properties of $\text{CH}_3\text{NH}_3\text{PbI}_3$ have not been investigated extensively. The theoretical study using density functional theory (DFT) by Xin Qian et al. [6] found a very low thermal conductivity (0.59 W/mK) for the tetragonal phase at room temperature, and higher thermal conductivity for the pseudocubic phase (1.80 W/mK) at 330 K. We systematically studied the elastic constants, vibrational properties and lattice

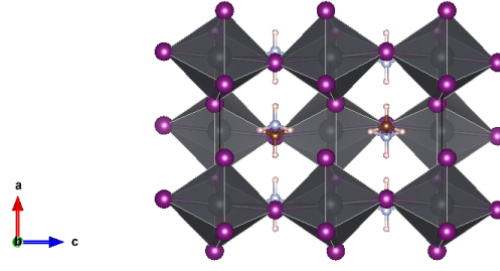


Figure 1. The crystal structure of the orthorhombic phase.

thermal conductivity of the $\text{CH}_3\text{NH}_3\text{PbI}_3$ in an orthorhombic system using density functional theory. The unit cell of the orthorhombic $\text{CH}_3\text{NH}_3\text{PbI}_3$, space group 62 (Pnma), with the unit containing 48 atoms is shown in Figure 1. The computational methodology of this study are elaborated in Section 2. Results and discussions are summarized in Section 3, and conclusions appear in Section 4.

2. Methodology

In this work, the investigation of the electronic structure properties was performed using the Vienna Ab-initio Simulation Package (VASP) [7, 8], based on Density Functional Theory (DFT) [9, 10]. The Projector-Augmented Wave (PAW) [11] method was employed to treat electron-ion interactions. To describe the electron exchange-correlation, we used the Generalized Gradient Approximation (GGA) as parameterized by Perdew, Burke and Ernzerhof for solids PBEsol [12]. $4 \times 4 \times 2$ Monkhorst-Pack meshes were used in sampling the Brillouin zone with an energy cut-off of 520 eV. The atomic positions were fully optimized until all components of the forces were less than 1 meV/atom.

To determine the stability of $\text{CH}_3\text{NH}_3\text{PbI}_3$ we examine its elastic constants. The elastic constants can be obtained by calculating the total energy as a function of the appropriate lattice deformation by first principles calculations. The elastic strain energy density is given by [13]

$$U = \frac{\Delta E}{V_0} = \frac{1}{2} \sum_i^6 \sum_j^6 C_{ij} e_i e_j, \quad (1)$$

where ΔE is the energy difference between the deformed and equilibrium structures; V_0 is the volume of cell; C_{ij} are the elastic constants; e_i and e_j are strains.

For an orthorhombic system, the nine independent elastic constants are $C_{11}, C_{12}, C_{13}, C_{22}, C_{23}, C_{33}, C_{44}, C_{55}$, and C_{66} . In terms of these constants, the Born conditions for mechanical stability [13] are

$$C_{11} > 0; C_{11}C_{22} > C_{12}^2; C_{11}C_{22}C_{33} + 2 C_{12}C_{13}C_{23} - C_{11}C_{23}^2 - C_{22}C_{13}^2 - C_{33}C_{12}^2 > 0; C_{44} > 0; C_{55} > 0; \text{ and } C_{66} > 0.$$

Bulk elastic properties: bulk modulus B_V , Young's modulus E and shear modulus G_V were calculated from the elastic constants by the Voigt method [14] using the following formulas for an orthorhombic crystal

$$B_V = \frac{1}{9}[c_{11} + c_{22} + c_{33}] + \frac{2}{9}[c_{12} + c_{13} + c_{23}] \quad (2)$$

$$G_V = \frac{1}{15}[c_{11} + c_{22} + c_{33} - c_{12} - c_{13} - c_{23}] + \frac{3}{5}[c_{44} + c_{55} + c_{66}] \quad (3)$$

The Young's modulus E , and Poisson's ratio, ν can be given by

$$E = \frac{9BG}{3B + G} \quad (4)$$

$$\nu = \frac{3B - 2G}{2(3B + G)} \quad (5)$$

Phonon properties were computed using a finite displacement method. Force constants were computed from a $2 \times 2 \times 2$ supercell expansion and analyzed using the Phonopy code [15] with VASP as force calculator. For the phonon density of states, the Brillouin zone (BZ) integrations were performed with $36 \times 36 \times 36$ meshes.

In general the thermal conductivity has two contributions, the electronic thermal conductivity κ_e and the lattice thermal conductivity κ_L . The lattice thermal conductivities were calculated with the single-mode relaxation-time (SMRT) approximation and linearized phonon Boltzmann equation as implemented in Phono3py [16]. For the third-order interatomic force constants a $2 \times 2 \times 2$ supercell was built containing 384 atoms, and reciprocal spaces of the supercells were sampled by $2 \times 2 \times 2$ meshes. To compute lattice thermal conductivity, the reciprocal spaces of the primitive cells were sampled using $8 \times 8 \times 8$.

3. Results and discussion

3.1. Elastic stability

The mechanical stability for $\text{CH}_3\text{NH}_3\text{PbI}_3$ orthorhombic crystal was obtained by checking that all the elastic constants are positive and satisfy the Born conditions for mechanical stability [13]. The computed elastic constants using PBEsol approximations are shown in Table 1. From the obtained results, one can confirm that the structure is mechanically stable against the influence of external forces in both approximations. Comparing our results from Table 1, with the values calculated from other work [5]. The differences in the values presented in Table 1 are due to the different approximation used.

Table 1. PBEsol calculated independent elastic constants for an orthorhombic system in (GPa)

Method	c_{11}	c_{12}	c_{13}	c_{22}	c_{23}	c_{33}	c_{44}	c_{55}	c_{66}
PBEsol	28.37	12.63	11.35	21.00	09.73	37.67	05.37	04.95	11.16
Other [5]	27.8	11.7	17.4	20.5	20.2	24.8	03.0	09.8	06.3

Table 2. Calculated bulk modulus B_V , Young's modulus E , shear modulus G_V , Poisson's ratio ν and B/G ratio

Method	$B_V(\text{GPa})$	$E(\text{GPa})$	$G_V(\text{GPa})$	ν	B/G
PBEsol	17.16	20.44	7.85	0.30	2.19
Other [5]	18.10	15.00	3.60	0.36	3.30

According to equations (2-5), the bulk modulus B , Young's modulus E , shear modulus G , Poisson's ratio ν and B/G ratio are presented in Table 2 with other theoretical results [5]. Our results show that the elastic constant C_{11} is smaller than C_{33} and larger than C_{22} for $\text{CH}_3\text{NH}_3\text{PbI}_3$, implying the anisotropy of its elasticity.

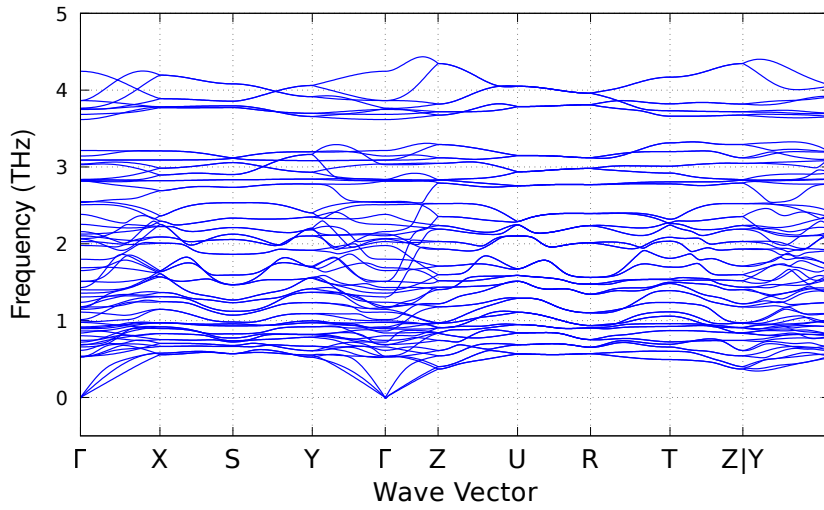


Figure 2. (Color online) Phonon dispersion relation graph calculated using PBEsol

3.2. Dynamical stability

Figure 2 shows the calculated phonon bandstructure curve of $\text{CH}_3\text{NH}_3\text{PbI}_3$ in an orthorhombic system. It can be seen from this figure that all phonon modes are positive in the Brillouin zone of the structure, therefore, the relaxed system is dynamically stable.

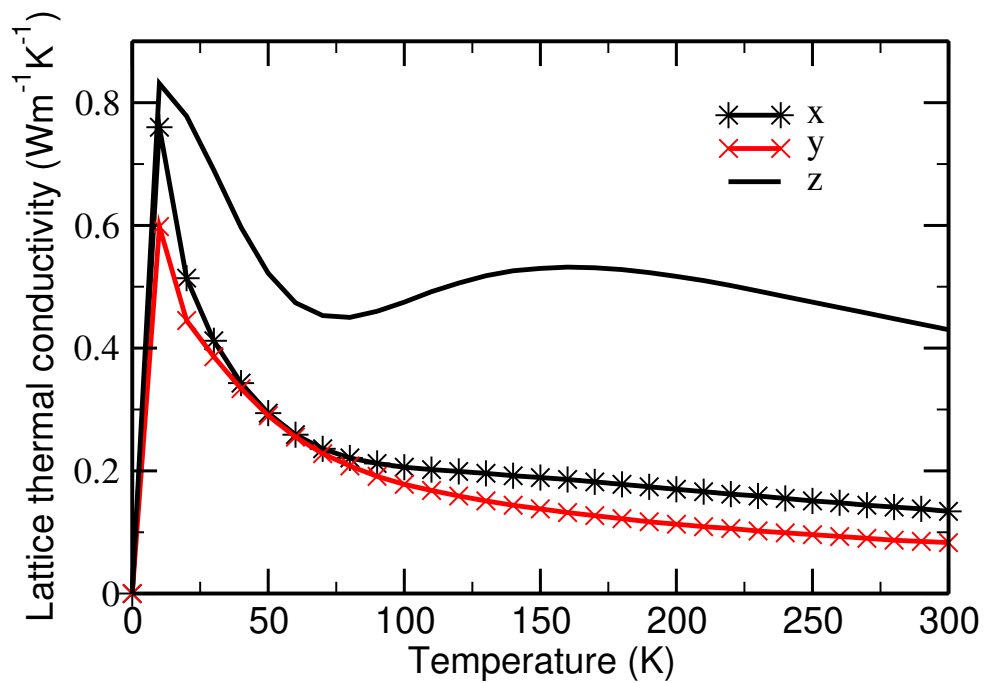


Figure 3. (Color online) Lattice thermal conductivity of $\text{CH}_3\text{NH}_3\text{PbI}_3$ as a function of temperature along x -, y - and z - axes.

3.3. Lattice thermal conductivity

The lattice thermal conductivity κ_L is very important which as it significantly affects thermoelectric material performance. Figure 3 shows the temperature-dependent lattice thermal conductivity κ_L of $\text{CH}_3\text{NH}_3\text{PbI}_3$ along x -, y - and z - directions. The calculated lattice thermal conductivities are found to be very low and anisotropic. For example, the calculated κ_L at 150 K along x -, y - and z - directions are 0.189, 0.138, and 0.530 $\text{Wm}^{-1}\text{K}^{-1}$, respectively. As temperature increases to room temperature κ_L reduces to 0.134, 0.083, and 0.43 $\text{Wm}^{-1}\text{K}^{-1}$ along x , y and z - directions, respectively. The obtained value on z direction is significantly larger than those values on the x - and y - directions. Table 3 shows the calculated lattice thermal conductivity for $\text{CH}_3\text{NH}_3\text{PbI}_3$ in an orthorhombic phase between 50 K and 150 K in the x -, y - and z -directions with the corresponding average values. At 150 K, the ratios $\kappa_L(z)/\kappa_L(y) = 3.84$ and $\kappa_L(z)/\kappa_L(x) = 2.80$, indicate high anisotropic behavior of the structure.

Table 3. The calculated lattice thermal conductivity ($\text{Wm}^{-1}\text{K}^{-1}$) in the x -, y - and z -directions with the corresponding average values.

T (K)	$\kappa_L(a)$	$\kappa_L(b)$	$\kappa_L(c)$	$\kappa_L(\text{avg})$
50	0.294	0.290	0.522	0.340
100	0.206	0.178	0.475	0.286
150	0.189	0.138	0.530	0.286

4. Conclusion

The structural stability, elastic constants, vibrational properties and lattice thermal conductivity of the orthorhombic $\text{CH}_3\text{NH}_3\text{PbI}_3$ have been calculated using a generalized gradient approximation as parametrized by Perdew, Burke and Ernzerhof PBEsol. The relaxed system is dynamically stable, and the equilibrium elastic constants satisfy all the mechanical stability criteria for an orthorhombic crystal, showing stability against the influence of external force. The calculated lattice thermal conductivity at 150 K was found to be 0.189, 0.138, and 0.530 $\text{Wm}^{-1}\text{K}^{-1}$ in the directions along x -, y - and z - axes, respectively. Our results confirmed the very low thermal conductivity.

Acknowledgements

IOAA would like to acknowledge the support he received from NRF-TWAS for funding, and Sudan University of Science and Technology (SUST). We also wish to acknowledge the Centre for High Performance Computing (CHPC), South Africa, for providing us with computing facilities.

References

- [1] Green M A, Ho-Baillie A and Snaith H J 2014 *Nature Photonics* **8** 506–514
- [2] Chen Q, De Marco N, Yang Y M, Song T B, Chen C C, Zhao H, Hong Z, Zhou H and Yang Y 2015 *Nano Today* **10** 355–396
- [3] Baikie T, Fang Y, Kadro J M, Schreyer M, Wei F, Mhaisalkar S G, Graetzel M and White T J 2013 *Journal of Materials Chemistry A* **1** 5628–5641
- [4] Brivio F, Frost J M, Skelton J M, Jackson A J, Weber O J, Weller M T, Goni A R, Leguy A M, Barnes P R and Walsh A 2015 *Physical Review B* **92** 144308
- [5] Feng J 2014 *APL Materials* **2** 081801
- [6] Qian X, Gu X and Yang R 2016 *Applied Physics Letters* **108** 063902
- [7] Kresse G and Hafner J 1993 *Physical Review B* **47** 558

- [8] Kresse G and Hafner J 1994 *Physical Review B* **49** 14251
- [9] Hohenberg P and Kohn W 1964 *Physical review* **136** B864
- [10] Kohn W and Sham L J 1965 *Physical review* **140** A1133
- [11] Kresse G and Joubert D 1999 *Physical Review B* **59** 1758
- [12] Perdew J P, Ruzsinszky A, Csonka G I, Vydrov O A, Scuseria G E, Constantin L A, Zhou X and Burke K 2008 *Physical Review Letters* **100** 136406
- [13] Mouhat F and Coudert F X 2014 *Physical Review B* **90** 224104
- [14] Voigt W 1928 *Ann Arbor, Mich*
- [15] Togo A and Tanaka I 2015 *Scr. Mater.* **108** 1–5
- [16] Togo A, Chaput L and Tanaka I 2015 *Physical Review B* **91** 094306